Ann. Geophysicae 14, 976–985 (1996)

Annales Geophysicae

On long-term evolution of seasonal precipitation in southwestern Europe

F. Valero, F. J. Doblas, J. F. González

Departamento de Física de la Tierra, Astronomía y Astrofísica II, Facultad de Ciencias Físicas, Universidad Complutense de Madrid, 28040 Madrid, Spain

Received: 28 June 1995/Revised: 25 January 1996/Accepted: 19 April 1996

Abstract. Annual cycles in long time series of precipitation from sixteen southwest European observatories have been analysed using complex demodulation. The stations have been clustered into two distinct regions and a hybrid one. They are referred to as the southwestern Europe precipitation Atlantic regime (SEPAR) and the southwestern Europe precipitation Mediterranean regime (SEPMER), with the hybrid regime referred to in terms of the mean amplitude ratios between semiannual and annual rainfall components. Some evidence of linking between seasonal cycle harmonic amplitudes and the zonal circulation has been found for SEPAR stations and a more obscured relationship for the SEPMER region. Within the SEPAR region the strength of the relationship is diminished towards the north. A trend analysis of the amplitudes against time since 1920 has also been carried out and the results reveal a divergent pattern in trends between annual and semiannual component amplitudes for the SEPAR region. In fact, both an increasing annual-amplitude trend and a decreasing semiannual-amplitude trend are observed, in each case statistically significant. The fact that the seasonal cycle variability of rainfall in southwestern Europe becomes more sensitive southwards to changes in atmospheric zonal circulation over the North Atlantic might, in our opinion, be related to the swing of the circumpolar vortex.

1 Introduction

Thomson (1995) has recently pointed out the evidence of a worldwide link between winter-summer temperature contrast and the climate change induced by greenhouse gases. Taking into account the physical relationship between the difference in the amount of solar energy that the Earth receives in winter and summer and the amplitude of the annual cycle in temperature, he finds that the likely role of solar energy on the climatic change is not as important as might be thought. Furthermore, tracking the annual cycle, he shows that there exists a general drift in the timing of the seasons (the date of the beginning of a "meteorological" year), which began around the 1940s, just when human-induced greenhouse warming appears to become stronger. This idea is based on the natural drift of one day per century, derived from the precession of the Earth, in the timing of the annual cycle. He also found variations in the timing of the annual cycle by studying northern-hemisphere records from about 1940. Moreover, by analysing both the temperature records in selected locations and the temperature averaged over the northern and southern hemispheres, he was able to identify an anomalous phase difference which accumulates over time and may even lead to reverse the sign of the natural phase drift of the annual cycle. This result is important because, according to Tabony (1984), the temperature contrast between seasons is related to the amplitude and phase of the annual cycle through the first and second harmonics. Generally, since the annual cycle accounts for a very important fraction of total variance of most meteorological variables, its time variations may have a non-negligible impact on atmospheric variability and therefore act upon the intra-annual (seasonal) variability and the timing of the seasons.

Climate may change in a wide range of potentially serious ways other than global warming. Precipitation can be considered one of the principal climatic elements to detect some likely climate change. Its high variability in time and space yields a low signal-to-noise ratio. Thus, evidence for any climatic change in precipitation becomes more difficult to detect than, for instance, that for the temperature itself. In fact, distribution of precipitation within a zonal belt is highly non-uniform and forces one to study this climatic element in a more restricted spatial setting.

Much of the variability in the extratropical atmosphere is directly associated with internal instability and

Correspondence to: F. Valero

non-linearity. A quantitative assessment of seasonal variability in the extratropics in general, and in regions such as Europe in particular, must rely on results from observational studies. We know that regional, including zonally averaged, climate variations often do not match those of the globe as a whole. Several large-scale analyses of precipitation changes over the northern and southern land masses have been carried out (Bradley *et al.*, 1987; Díaz *et al.*, 1989). They have demonstrated that during the last few decades precipitation has tended to increase in the mid-latitudes, but decreases in the northern-hemisphere subtropics and generally increases throughout the southern hemisphere. However, these large-scale features contain considerable spatial variability. Southwestern Europe straddles mid-latitudes and subtropics, and so involves greater uncertainty in precipitation time and space patterns.

Annual cycle evolutions have often been studied through harmonic analysis applied on overlapping and non-overlapping data subsets (Manley, 1974; Smith, 1984). More recently, the use of powerful tools to handle variables with a very poor signal-to-noise ratio, such as precipitation, has been seen to be successful. A preliminary observational study on long-term seasonal evolution of precipitation is carried out in this paper by means of a powerful tool called complex demodulation. Estimates in time domain of amplitude and phase for a fixed-frequency signal are obtained in attempting to find out their corresponding time evolutions. The main advantage of our approach is, as was argued by Thomson (1995), that it is a method which is able to work even with quite noisy time series.

Section 2 describes the data sets used. Section 3 consists of a background review of complex demodulation. The main systematic and repeatable differences in the characteristics of amplitude and phase time series from the individual observatories are described in Sect. 4, and in Sect. 5 some comments and conclusions are highlighted.

2 Data

Sixteen long time series of monthly precipitation have been used in this paper. Table 1 lists the latitude and longitude coordinates (with negative values to the west of Greenwich meridian), the sampling period and the total number of missing data for each station as well as their proportion in percentage (in parenthesis). Twelve of them are observatories spread over the Iberian Peninsula and the Balearic Islands. The other four observatories are sited over southwestern Europe. Two of them, Bordeaux and Marseille, have been reconstructed from several original recorded time series, provided by Météo-France, using the Durbin-Watson method described in Valero *et al.* (1996).

One important consideration in the selection of time series for analysis is the amount and distribution of missing data. After examination of the available datasets and the distribution of missing values in these datasets, some information about this issue is shown in Table 1. Some of the series contained gaps, but these did not exceed 3% of the total data in any case. Missing data become a lesser problem when the gaps are well scattered, as is the case here. Each missing datum was interpolated by averaging data for the same month of the three years previous to and three years following the gap. This procedure has a drawback in the case when gaps exist within a 3-year data segment either at the beginning or at the end of the record. In such a case, some data of the segment have been necessarily excluded.

Table 1. List of stations where monthly precipitation records have been studied. The table contains the geographic coordinates (latitude and longitude) and the first and last year of the studied period. The extreme right-hand side column denotes the total number of missing data as well as its percentage (in parenthesis)

Station	Lat.	Long.	Period	Missing data
Alicante (AL)	38°22′	− 0°30′	1899–1993	3 (0.3)
Badajoz (BA)	38°53′	− 6°58′	1899–1984	2 (0.2)
Bologna (BO)	44°°30′	11°18′	1813–1990	0 (0.0)
Bordeaux (BD)	44°25′	− 0°40′	1848–1994	0 (0.0)
Burgos (BU)	42°20′	− 3°42′	1899–1990	28 (2.6
Coruña (CO)	43°20′	− 8°25′	1899–1989	2 (0.2)
Granada (GR)	37°10′	− 3°42′	1899–1976	3 (0.3)
Jean (JA)	37°48′	3°48′	1899–1985	23 (2.2)
Madrid (MA)	40°25′	− 3°45′	1899–1991	2 (0.2)
Marseille (MS)	43°26′	5°12′	1749–1993	0 (0.0)
Milan (MI)	45°27′	9°11′	1764–1990	0 (0.0)
Murcia (MU)	37°59′	− 1°08′	1899–1980	14 (1.4)
Palma Mallorca (PM)	39°34′	2°39′	1899–1993	0 (0.0)
San Fernando (SF)	36°28′	− 6°12′	1899–1987	5 (0.5)
San Sebastian (SS)	43°19′	− 2°03′	1899–1994	0 (0.0)
Sevilla (SE)	37°23′	− 5°59′	1899–1993	17 (1.5)

Finally, the time series of mean sea-level pressure differences between Ponta Delgada, Azores and Akurery, Iceland from 1867 to 1989 has been tackled. This series can be viewed as an index of the North Atlantic oscillation (NAO) pattern (Rogers, 1984; Lamb and Peppler, 1987).

3 Estimating amplitude and phase

The signal processing method known as complex demodulation can be applied to any time series. The aim of the complex demodulation is to extract information about a perturbed periodic component with slowly varying amplitude and phase. Such information consists of the time variation of the amplitude and phase of any non-stationary component of selected frequency. The analysis is similar to harmonic analysis in that the amplitude and phase are described, but different in that the amplitude and phase are determined only by the data in a local time interval rather than by the whole series. An excellent description of complex demodulation is given by Bloomfield (1976).

For brevity, we shall only present the continuous-time formulation herein. A time series, $x(t)$, embedding an oscillation of ω frequency with a slow-time-varying amplitude and phase, $A(t)$ and $\Phi(t)$, respectively, can be expressed as:

$$x(t) = A(t)\cos(\omega t + \Phi(t)). \quad (1)$$

This oscillation may be merged with a noisy (non-periodical) term $R(t)$ without any component at frequency ω. In such a case, it can be rewritten as

$$x(t) = A(t)\cos(\omega + \Phi(t)) + R(t). \tag{2}$$

Complex demodulation consists mainly of two steps clearly illustrated by Humphries and Restrepo (1992). First, carrying out the shifting of the spectral density associated with the frequency ω to the zero frequency by multiplying the series $x(t)$ by $e^{-\omega t}$. Second, filtering out the resulting time series through a complex low-pass filter. Having applied this methodology, a new shifted and filtered complex time series $u(t)$ is obtained

$$u(t) = \int_{-\infty}^{+\infty} h(s)x(t-s)e^{-i\omega(t-s)}\,ds, \tag{3}$$

where $h(s)$ is the impulse response function of the filter or the weight function of the time-invariant linear system, which provides a description of the system in the time domain. The frequency response function $H(\omega)$ or transfer function is the Fourier transform of the impulse response function. This is a complex function and can be expressed as

$$H(\omega) = G(\omega)e^{i\gamma(\omega)}, \tag{4}$$

where $G(\omega)$ is the gain which is a measure of the changing amplitude of ω-frequency components and ranges between -1 and 1; $\gamma(\omega)$ is the phase shift. Note that if $R(t)$ has any frequency different from ω, it will be removed by the idealized low-pass filter in Eq. (3), because in this case $G(\omega)$ is a delta-shaped function.

Both amplitude and phase time series are given, respectively, by

$$A(t) = 2\|u(t)\|, \tag{5a}$$

$$\Phi(t) = \arg(u(t)), \tag{5a}$$

the operator $\|\ \|$ being the quadratic norm $[(\mathrm{Re}(u(t)))^2 + (\mathrm{Im}(u(t)))^2]^{1/2}$, and arg( ) the $tg^{-1}[\mathrm{Re}(u(t))/\mathrm{Im}(u(t))]$

Since in the current case the time series are discrete and of finite length, the low-pass filter ought to have a discrete impulse response function and hence a finite number of coefficients; that is to say, the theoretical frequency response function will have to be transformed into an empirical function with a maximum at ω. Accordingly, a frequency band rather than a single frequency is involved in the process (Enting, 1987). For $\Phi(t)$ not constant, two possibilities can arise. One is that either a linear fall or rise in time does occur. In this case, the signal frequency is not exactly determined but may still be obtained, as presented in Thomson (1995), by adding the initial frequency to the slope of the straight line fitted to the phase time series. On the other hand, the phase can vary almost randomly in time; here the variability results from those components $R(t)$ with frequencies very near to ω in Eq. (2) which are included within that spectral band inherent in the filter resolution. Fortunately, the variance of the 12- and 6-month period components is large enough when compared with the background noise.

In this paper, the least-square low-pass filter as defined in Bloomfield (1976) is used. The discrete impulse response function is given by

$$h_0 = \frac{\omega_c}{\pi},$$

$$h_u = \frac{\sin(u\delta)/2}{u\delta/2}\,\frac{\sin u\omega_c}{\pi u}, \tag{6}$$

where ω_c is the cutoff frequency and δ is the wavelength of the Gibbs-phenomenon (a characteristic of the truncated Fourier series of a discrete function) ripples originated by any discrete filter. The value of δ depends on the filter length k as

$$\delta(k) = 4\pi/(2k+1). \tag{7}$$

Most of the decay from the passband to the stopband in the gain takes place over a range of δ, and also depends inversely on filter length. Thus, the larger k is, the larger the rate of decaying is, thereby a lesser number of components close to ω are included in the filtering. With this filter the negative influence of the Gibbs phenomenon on the gain is greatly reduced and the phase $\gamma(\omega)$ kept unchanged. The advantage of this filter lies mainly in its behaviour near $\omega = 0$, where the gain is close to 1 (ensuring that virtually all the signal is passed) and slowly varying (so that different frequencies contributing to the peak are treated equivalently).

Features of the filter are given by two parameters: (i) the pass frequency ω_p (last frequency with gain equal to 1), and (ii) the stop frequency ω_s (first frequency with gain equal to 0).

4 Results and discussion

Complex demodulation is used here to analyse the presumed changes in amplitude and phase of seasonal precipitation cycle during the current century of 16 long monthly rainfall records.

An inspection of monthly rainfall periodograms in Fig. 1 reveals the annual cycle in two main ways or spectral modes: a first spectral mode for the case where 12-month component exceeds 6-month component (as depicted in Fig. 1a), and a second mode for the case in which 6-month component exceeds 12-month component (as depicted in Fig. 1b). The first and second harmonics account for most of the annual variance, in good agreement with the results of the comprehensive study of Hsu and Wallace (1976).

By observing in detail the first and second columns in Table 2, the stations may reasonably well be clustered in terms of each spectral mode or, analogously, by means of the ratios between semiannual and annual amplitude components. Those stations associated with ratios equal or greater than 1 obey a southwestern Europe precipitation Mediterranean regime (SEPMER), and those having a ratio lower than 1 are classified as being in a southwestern Europe precipitation Atlantic regime (SEPAR). For practical purposes, stations were clustered according

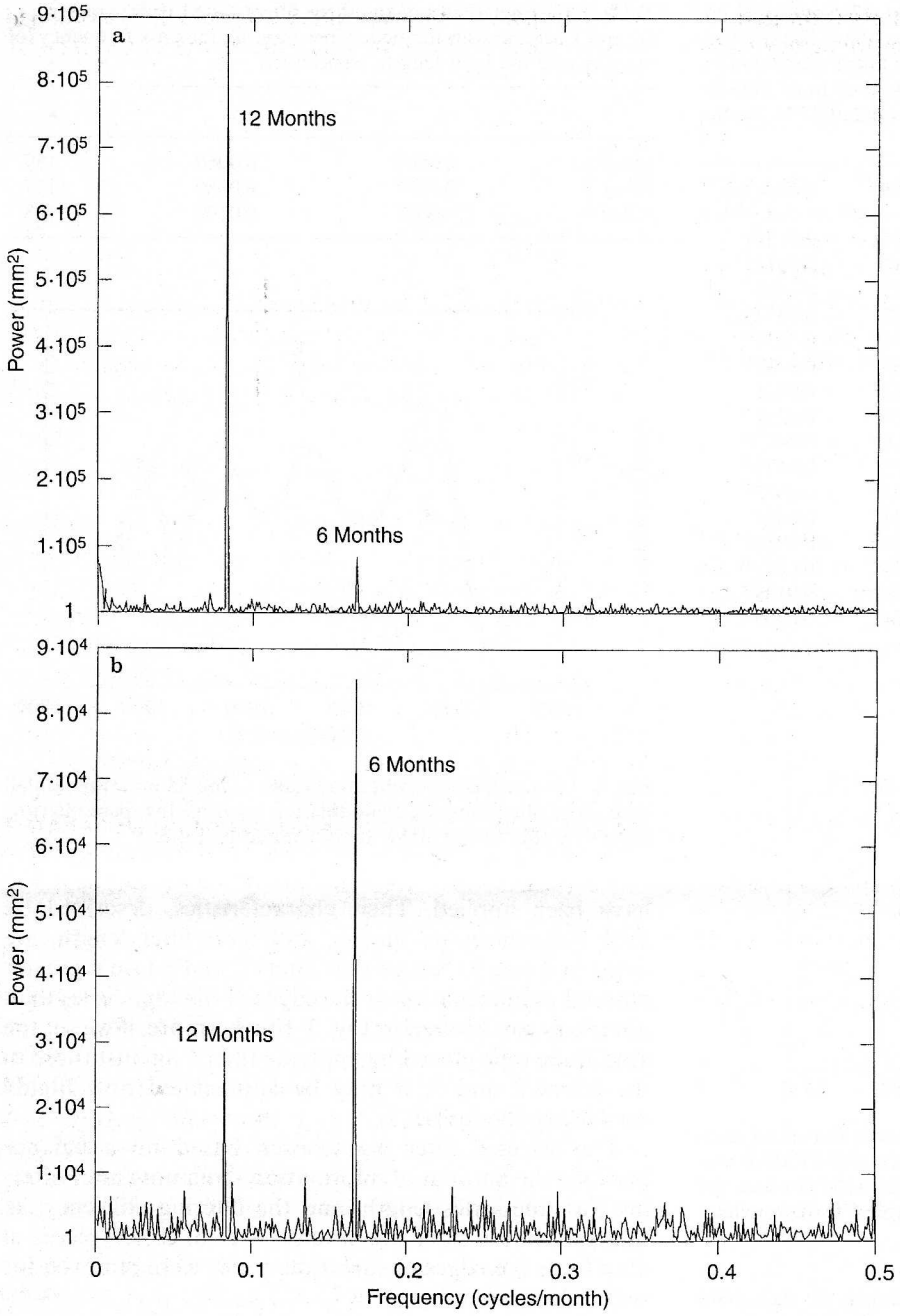

Fig. 1a, b. Periodogram of the **a** Coruña and **b** Murcia monthly rainfall time series. The 12- and 6-month periodicities stand out as peaks in the spectrum

to three major categories in terms of ratio values, namely:
- ratios less than or equal to 0.85 (SEPAR),
- ratios from 0.86 to 0.99 and
- ratios greater than 1 (SEPMER).

The threshold value of 0.85 was set in accordance with the issues derived from a comprehensive factor analysis of Iberian precipitation by Villa *et al.* (1985). Such a critical value was obtained by "tuning" ratio values so that SEPAR and SEPMER rainfall patterns were really much the same as those from Villa *et al.* (1985). By doing so, two stations, Madrid (MA) and Marseille (MS) (denoted by open circles in Fig. 2), exhibit a somewhat mixed pattern. Also in Fig. 2, ratios lower than 0.85 (solid circles) are found over much of the Iberian Peninsula and southwestern France associated with SEPAR-type stations, whereas ratios greater than 1 (solid triangles) linked to SEPMER-type stations fill southeastern Spain and northern Italy. There are two stations which do not exhibit the expected pattern: Burgos (BU), which is SEPMER instead of SEPAR as might have been expected, and Palma (PM), which SEPAR instead of SEPMER.

Ratios lower than 0.85 are representative of annual courses with only one wet and one dry season. It is evident that when the annual component is remarkably superior to the semiannual component, only a maximum and a minimum occur. In a similar manner, when ratios are greater than 1, rainfall throughout a year may be decomposed into both two wet and dry seasons.

Table 2. The averaged amplitudes (in mm) for 12-month and 6-month period components are listed in the first column. The two last columns show the slopes (in mm/month) of the linear regression in time for both 12- and 6-month component amplitude from 1920 to the end of the record. Significant slopes at the nominal 0.1% significance level are marked by *asterisks*

Station	12-months	6-months	Slope (12)	(Slope (6)
AL	9.8	22.8	−0.0024*	0.0102*
BA	27.7	11.2	0.0182*	−0.0083*
BO	10.7	20.3	−0.0038*	−0.0016
BD	18.4	11.6	0.0024*	−0.0043*
BU	10.8	12.6	0.0044*	−0.0136*
CO	42.0	13.2	0.0109*	−0.0097*
GR	24.4	13.4	0.0162*	−0.0021
JA	37.7	13.4	0.0078*	−0.0261*
MA	13.8	13.3	0.0076*	−0.0072*
MS	21.4	21.6	−0.0005	−0.0176*
MI	13.1	20.9	0.0034*	−0.0072*
MU	7.8	13.7	−0.0051*	0.0019
PM	18.8	15.9	−0.0078*	−0.0036*
SF	43.4	14.0	0.0224*	−0.0047*
SS	34.6	21.0	−0.0087*	−0.0139*
SE	38.8	13.5	0.0184*	−0.0203*

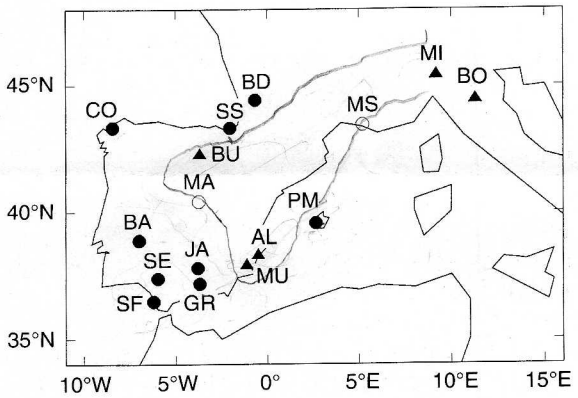

Fig. 2. Geographical arrangement of southwestern European rainfall spectral modes. First (SEPAR stations), second (SEPMER stations) and hybrid spectral modes are denoted by *solid circles*, *solid triangles*, and *open circles*, respectively. See Table 1 for acronyms

In indication of the skill of the clustering we can note that, for instance, Alicante (AL) and Murcia (MU) observatories show very high ratios (about equal to or greater than 2) against the Granada (GR) station which shows a ratio markedly lower than 1. This result agrees well with the issues argued by Valero *et al.* (1993) in a more locally detailed study conducted for southeastern Spain using cross-spectral analysis. After searching for the influence of the Atlantic climate along the Mediterranean coast, they have showed a progressive change along the coast line in the ratio between the spectral densities associated with the two aforementioned harmonics.

The complex demodulation of the precipitation series, was carried out using a variety of low-pass filter lengths. To evaluate the performance of low-pass filtering in extracting the yearly range of the annual cycle, San Sebastian's (SS) rainfall time series was chosen because no missing data exist within it. Three different low-pass filters

Table 3. Characteristics of the three filters tested in this paper. ω_s, ω_p and k are the stop-frequency (per month), the pass-frequency (of month), and the filter length, respectively

	ω_s	ω_p	k
Filter 1	0.0007	0.0060	189
Filter 2	0.0007	0.0080	137
Filter 3	0.0007	0.0100	108

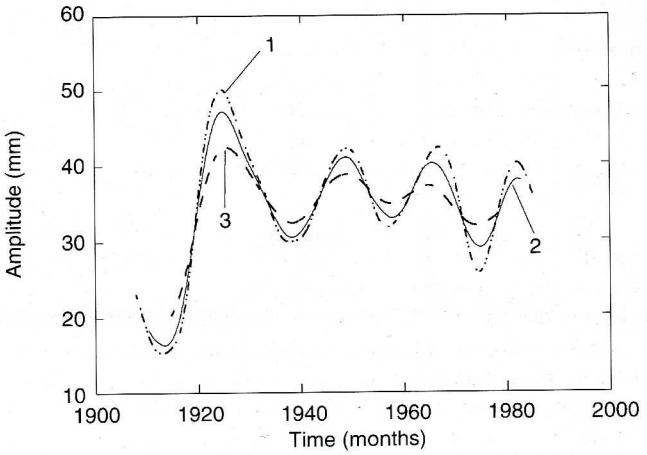

Fig. 3. 12-month component amplitudes of the SS monthly rainfall time series after complex demodulation for three low-pass filtering. Characteristics of the filters are illustrated in Table 3

have been applied. Their characteristics, described by their frequencies ω_p and ω_s and their filter length, are listed in Table 3. Notice that filters 2 and 3 lose a greater amount of information at the edges of the time series than filter 1, as can be seen in Fig. 3. Furthermore, if we set the amplitude reproduced by applying filter 1 against those of the filters 2 and 3, it may be appreciated how highly oscillatory the former is.

The selected filter was chosen based on a balance between the amount of information remaining after filtering (or time-series length) and the filtering efficiency, so that the chosen filter was filter 2. A total of 136 pieces of data from the edges of each time series were removed for such a low-pass filter.

4.1 Annual component

As can be seen in Fig. 4, the amplitudes of the 12-month precipitation component do not present a uniform but rather a relatively high oscillatory behaviour throughout the studied time interval. Another general aspect is the amplitudes' greater variability in both time and space when compared with those of Thompson (1995) for the 12-month temperature amplitudes. Considering that the used filter is very similar to that in Thompson's paper, these differences in the range of amplitude variability should not entirely be attributed to the characteristics of our filter, but rather to the nature of precipitation data and the characteristics of the region under study. However, as stated in Sect. 3, the reader should bear in

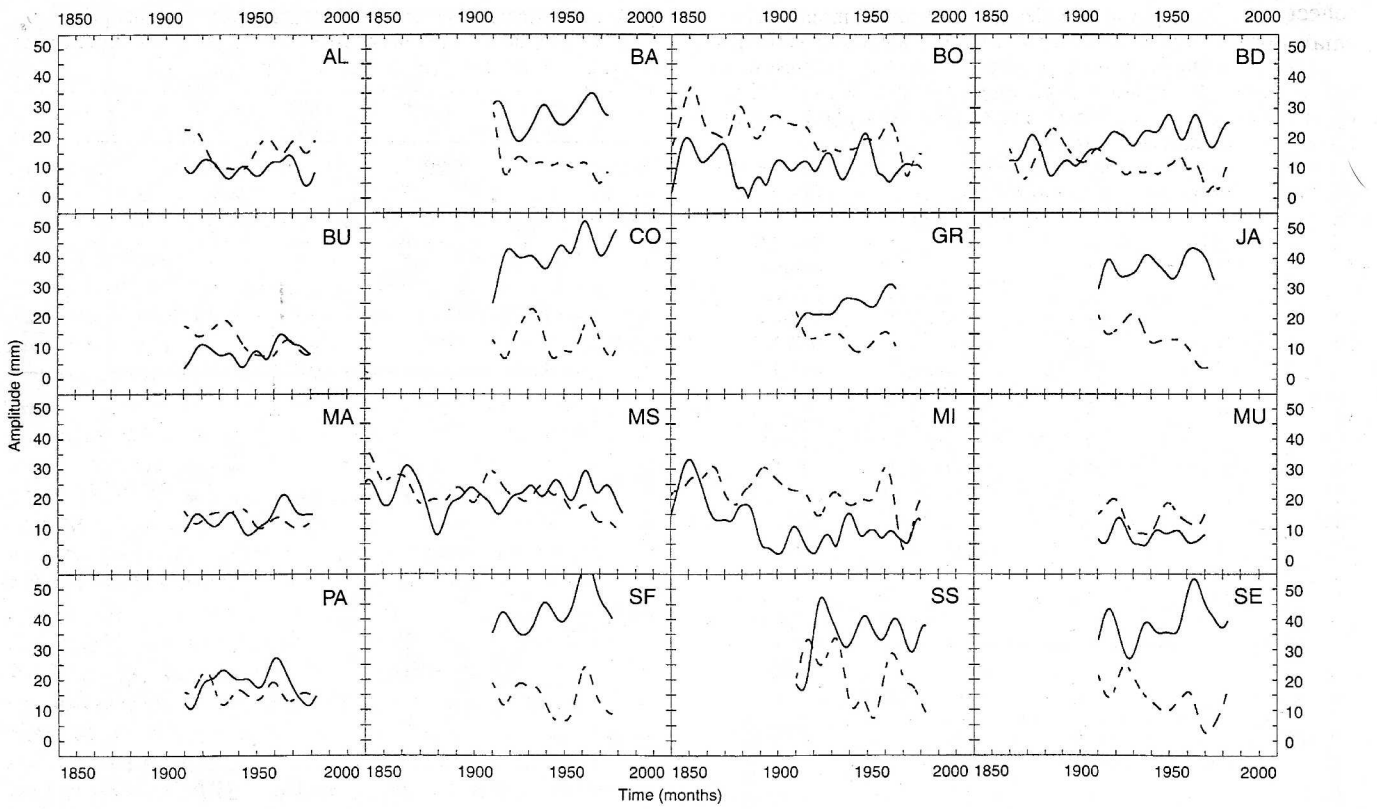

Fig. 4. Annual (*solid lines*) and semiannual (*dashed lines*) component amplitudes of the sixteen monthly rainfall time series. See Table 1 for acronyms

mind that the filtering process might give rise to spurious oscillations both in the amplitude and phase outcomes. Such spurious oscillations would arise from the fact that we are not demodulating a single frequency but a frequency interval. In other words, the gain of the filter is not a delta function but a function that involves a band of frequencies. Therefore caution must be taken when interpreting demodulation outcomes. Despite such a handicap, the amplitude variations of the 12-month and 6-month waves for different stations show reasonably high consistency, and so some conclusions may be drawn.

An overview of Fig. 5a roughly reveals that stations in the southwestern Iberian Peninsula (Badajoz (BA), Granada (GR), Jaen (JA), Sevilla (SE), San Fernando (SF)] undergo similar oscillations in the annual component amplitude with minima in the 1920s and around 1950. Also, maxima emerge in the 1910s, around 1940 and the 1960s. The amplitude changes in the annual variations repeat in these stations as a pattern-like highly consistent arrangement. It is also noticeable that the consistency of this oscillation pattern becomes progressively weakened eastward, so that, for southern stations (AL, MU), such a pattern is practically absent. Northern stations, however, reveal a somewhat different pattern to southwestern Iberian Peninsula stations. It may be asserted by viewing Fig. 5b that stations Coruña (CO), San Sebastian (SS) and Bordeaux (BD) also exhibit a structure in the form of maxima and minima. Noticeable maxima are mainly located around 1920, 1950, in the 1960s and 1980s. In contrast, minima arise in the early 1940s (except for BD where the date is 1930), the 1950s and the 1970s.

The remaining stations, i.e. MU, AL, MS, Milan (MI), Bologna (BO), PM and MA, do not reveal a consistent enough pattern either among themselves or with the northern and southern patterns, even though MU and AL match each other reasonably well. Such between-station differences require further study in order to gain some more understanding on such typical, at least geographically, Mediterranean stations.

Zonal indices are one of the most frequently used parameters for characterizing the type of circulation over any given geographical area. The most commonly used is the mean sea-level pressure difference between two different latitudes in such a manner that the circulation varies between a high index or zonal type, and a low index or meridional type. We have herein used the well-known pressure difference between the Azores anticyclone and the Iceland low. Our index of westerly flow is expressed as the difference in atmospheric mean sea-level pressure (DAP) between Ponta Delgada, Azores and Akurery, Iceland (Rogers, 1984). Its long-term evolution is shown in Fig. 5c after low-pass filtering of DAP time series. High index involves stronger or more frequent westerly flow across the extratropical North Atlantic than low index. Figure 5c shows the DAPA (annual component amplitude in DAP) after applying the same filter as for the other complex demodulates. Interdecadal variations of DAPA are remarkably large, with maxima around 1910, 1930,

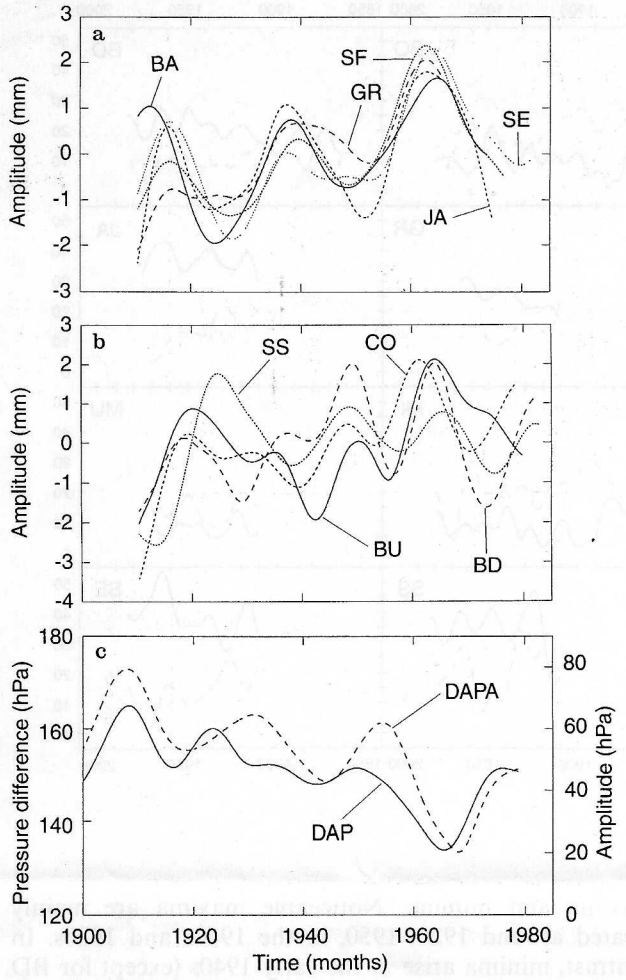

Fig. 5a–c. Standardized annual component amplitudes of **a** southern SEPAR-station rainfall, **b** northern SEPAR-station rainfall and **c** DAP (DAPA12), monthly time series. *Solid line* in **c** represents low-pass filtered DAP time series. See the text for filter features and Table 1 for acronyms

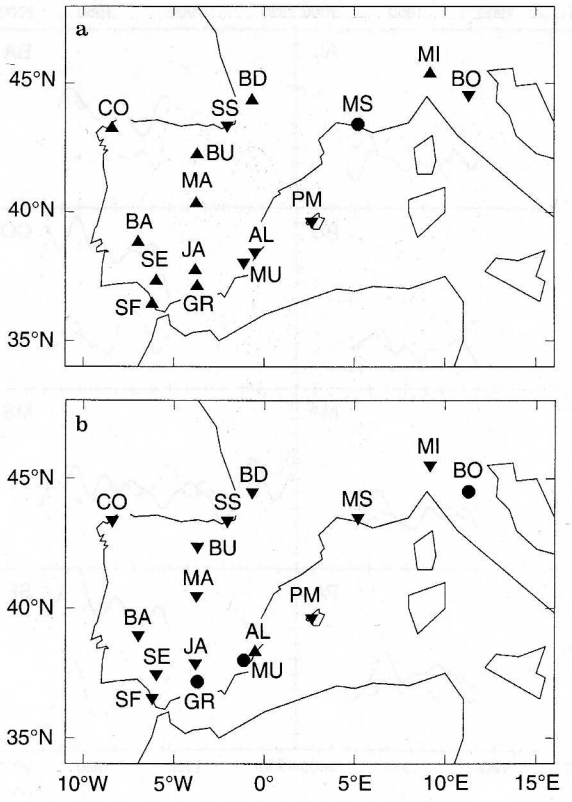

Fig. 6a, b. Slopes after 1920 for **a** 12-month and **b** 6-month amplitude components. *Upward* (*downward*) *solid triangles* mean positive (negative) statistically significant (99% confidence level) slopes. *Solid circles* denote statistically non-significant slopes. See Table 1 for acronyms

late 1950, as well as recently, in great accordance with Flohn *et al.* (1990).

Maheras (1988) pointed out two principal moist periods (1901–1921 and 1930–1941) and two principal dry periods (1922–1929 and 1942–1954) derived from a principal-components analysis of precipitation in the western Mediterranean. He claims that the first moist period corresponds to a small decrease in the western zonal circulation, while the second moist period coincides with a characteristic minimum of the zonal circulation (see Fig. 5c). On the other hand, the first two dry periods coincide with a reinforcement of the zonal circulation. It is noticeable that the curves in Fig. 5a evolve following such a pattern. In contrast, the curves in Fig. 5b are nowhere near as similar to Maheras' pattern as those for southern SEPAR (Fig. 5a). Therefore it can be argued that maxima in amplitude for the southern set are reasonably coincident with low zonal circulation periods, and vice versa. In support of the above thesis, correlations among the filtered DAP and 12-month amplitude precipitation time series have been obtained after having removed a linear trend. Correlation values are found to be highly negative for southern SEPAR stations (BA: −0.55, GR: −0.46, JA: −071, SF: −0.79 and SE: −0.74), and to a rather lesser extent for the northern SEPAR set (BD: −0.47, CO: −0.28 and SS: 0.05). The negative correlations confirm the results of Maheras (1988). The inescapable conclusion is that meridional circulation drives higher values both in the amplitude of the annual component and the annual precipitation in southwestern Iberian Peninsula.

It is well worth noting that DAP and DAPA time series (Fig. 5c) are well correlated (0.61 at zero-lag), albeit that correlation rises to 0.74 when DAPA series is lagged 29 time units. The physical mechanism responsible for this delay remains unknown.

Least-square linear regressions of the 12-month component amplitudes against time after 1920 have been computed and their slopes are presented in Table 2. The choice of this date is based on reported changes in circulation (Loewe, 1937; Winstanley, 1973b) over the northern Atlantic Ocean and western Europe after the 1920s. In accordance with these features, Pfister (1992) reveals that the maritime period of the 1920s presents by far the most extreme change in continentality since the year 1535, and since then some trend has been noticed. A significance *t*-test (Snedecor and Cochran, 1967) for constant amplitude was applied. As amplitude time series present a strong autocorrelation, values are not independent of each other and the effective number of data has been

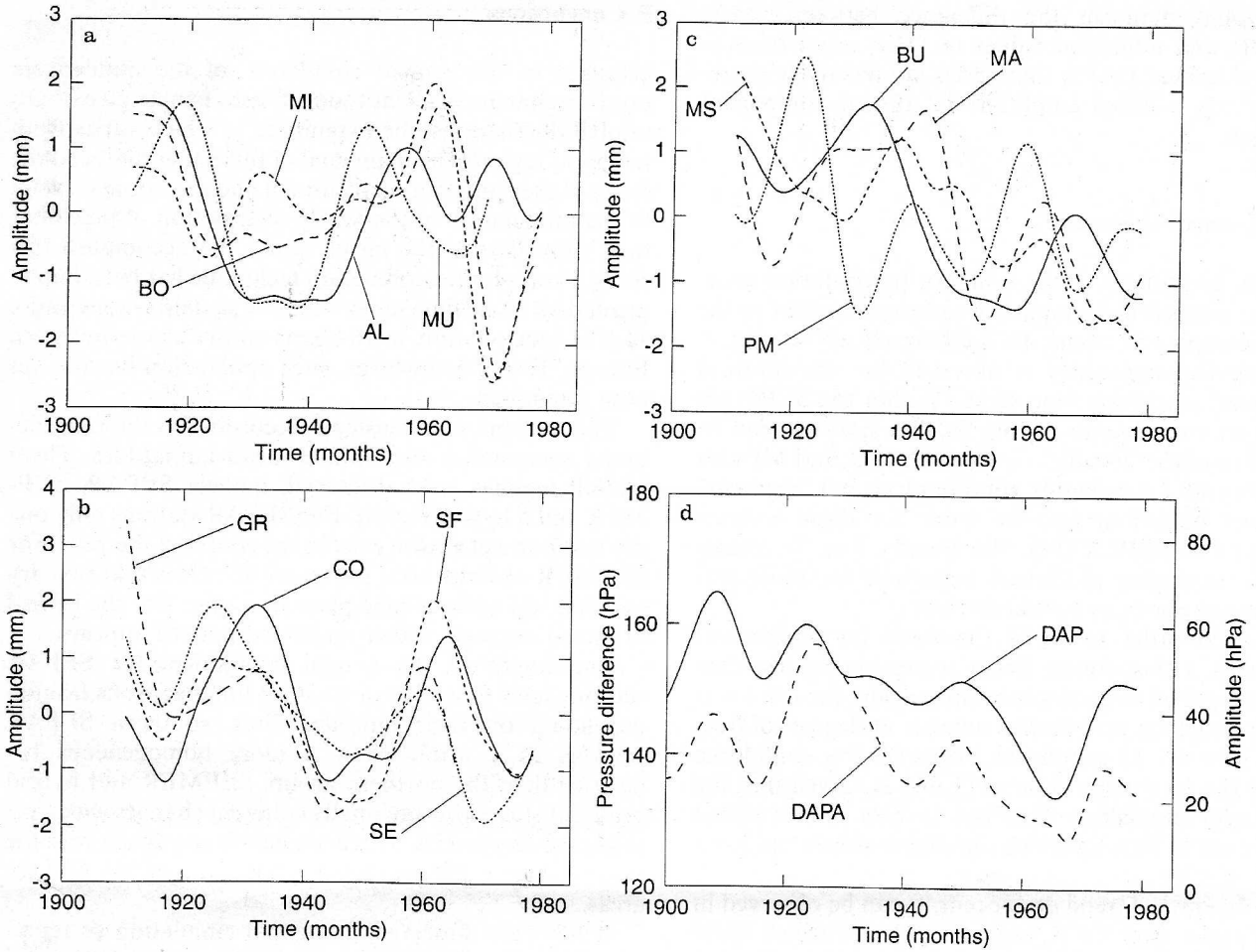

Fig. 7a–d. Standardized semiannual component amplitudes of **a** SEPMER-station rainfall, **b** SEPAR-station rainfall, **c** hybrid-station rainfall and **d** DAP (DAPA6) monthly time series. *Solid line* in **d** represents low-pass filtered DAP time series. See the text for filter features and Table 1 for acronyms

computed following Trenberth (1984). Of the 16 slopes, 15 prove significant (99.9% confidence level), as can be seen in Table 2 and Fig. 6a. In order to test how significant these results are, in other words, how likely it is that a series with strong annual amplitude and a white-noise interannual evolution of this amplitude will present similar patterns, a number of Montecarlo simulations have been performed. Indeed, eight simulations, made up of:

- generation of one thousand synthetic time series,
- complex demodulation of each time series and
- trend analysis of the amplitudes

were carried out. The first stage obeys the following equation

$$x_t = \left(A_1 + \frac{A_{2t}}{D} \cos \frac{t}{\mathrm{PER}}\right) \cos \frac{l}{12}, \tag{8}$$

where A_1 is the mean amplitude, A_{2t} is a white-noise time series (zero mean and unit variance) different for each time series, D is a scaling term and PER is the period of the amplitude interannual variation. Each simulation involved fixed values for these parameters, which ranged between 10 and 20 units for A_1, 200 and 1000 for D, and 100 and 180 time units for PER, according to the observed amplitude features. Results showed that between 22% and 36% of the synthetic time series generated in each simulation had spurious significant (99% confidence level) non-zero slope in their amplitude time series. If we set 15/16 significant non-zero slopes in observed data against a maximum of 36% obtained in simulation outcomes, it is beyond all doubt that this result is not the consequence of chance.

Positive trends are associated to SEPAR stations (except for SS) and negative trends to SEPMER stations (except for MI), as shown in Fig. 6a. Generally, positive slopes for SEPAR observatories are over 0.0100 mm/month. Nevertheless, a statistically significant negative slope (−0.0429 hPa/month, 99.9% confidence level) has been found for annual DAPA series, which might be related to the inverse correlation between 12-month precipitation amplitude in SEPAR stations and annual DAPA time series. Related to this fact is the idea presented by Winstanley (1973b). He affirms that the strength of the westerly circulation reached a peak in the mid-1920s, and that it has been decreasing since then. The fall in westerly strength could be related to a decrease in mean sea-level pressure difference between 30°N and 60°N. This

effect would diminish the difference between yearly maximum and minimum values in DAP series because DAP and annual DAPA time series are positively correlated, giving a lesser amplitude in annual component amplitude.

4.2 Semiannual component

As far as amplitudes of the 6-month precipitation component are concerned, amplitude variations similar to the annual component occur. By looking closely at Fig. 7, some regional coherency is observed for standardized semiannual amplitude time series. Within the SEPMER scheme we can observe in Fig. 7a that stations tend to oscillate in-phase "locally", i.e. AL with MU, and MI with BO. However, a reasonably good in-phase but "regional" oscillatory behaviour may be found for those stations referred to as SEPAR (Fig. 7b). Finally, Fig. 7c reveals a rather uncoupled oscillatory behaviour for those stations named above as hybrid stations.

Again, in order to check the trend for semiannual amplitudes, a least-square linear regression against time has been applied to each series. Once again, the *t*-test was also corrected for the effective number of degrees of freedom. There are 13 significant slopes (99.9% confidence level) in the 16 studied stations (Table 2). Given that the Montecarlo simulation described in Sect. 4.1 provided a maximum of 36% spurious significant slopes, the ratio of 13/16 significant trends supports our argument that an overall downward trend does occur. It can be observed in Table 2 that after 1920, only two observatories show non-negative slopes. These two observatories, AL and MU, are located on the Spanish Mediterranean coast. Furthermore, a non-significant slope is shown by BO. Thus, SEPMER stations show either positive or negative slopes, which is a straightforward consequence of Mediterranean climatology. Indeed, in support of this argument it is worth highlighting that convective and local phenomena, typical of this region, have a stronger effect on rainfall distribution throughout the year than in the Atlantic region. This effect could explain the relatively increased importance of the semiannual component with regard to the annual rainfall component. In other words, we think that the 12-month cycle is very likely to be dominated by the large-scale dynamics, while the 6-month component is presumably more seriously affected by the thermodynamics and by the vertical structure of the atmosphere. The stations characterized by SEPAR and hybrid regime all present negative slopes (Table 2). The fact that the 6-month DAPA and the DAP series do not show appreciable correlations with the 6-month rainfall amplitudes points out this somewhat more local character of the 6-month component. In addition to these precipitation features, a decrease (-0.0502 hPa/month, significant at 99.9% confidence level) in the 6-month DAPA time series (Fig. 7d) since 1920 is also clear. Precipitation amplitude trends seem to depend on the place of the observatory with respect to the Atlantic influence on climate, but they are almost always lower than -0.0030 mm/month, i.e. -0.036 mm/year.

5 Conclusions

Changes in the general circulation of the atmosphere produce changes in all latitudes. These changes give rise to rainfall fluctuations, the magnitude of which varies from region to region. The main goal of this paper has been the study of the contribution of annual and semiannual cycles to the modulation of the yearly distribution of precipitation, regardless of the mean values. To accomplish this study a complex demodulation technique has been implemented for some time series with low signal-to-noise ratio, such as precipitation, in 16 observatories in southwestern Europe. To our knowledge, such application has not yet been attempted.

The stations were clustered according to the ratio between semiannual and annual mean amplitudes. Three rainfall regimes were discerned, namely SEPAR, SEPMER and a hybrid regime. For SEPAR stations only one dry and one wet season exist in the course of the year. For SEPMER observatories the major feature is that two dry and two wet seasons take place in a year. For the hybrid or mixed regime a rather undefined pattern appears.

Amplitudes of the annual component for SEPAR stations tend to evolve in a rather homogeneous fashion depending on their latitude. Thus, southern SEPAR stations as a whole show a more homogeneous behaviour than the northern group. SEPMER and hybrid groups do not show regionally coherent changes with time in annual amplitudes. This argument is consistent with the lower values of the yearly component amplitude in these areas.

It has been observed that zonal circulation as represented by the DAP index is closely related to annual precipitation amplitude variations in southwestern Iberian Peninsula, while it is obscured for the remainder of the studied regions. A physical plausible mechanism to link the annual component amplitude and the zonal circulation could well perform as follows: when the annual DAPA is less than normal, i.e. when smaller autumn-winter and/or greater DAP than normal for summer is observed (Fig. 2, Makrogiannis *et al.*, 1991), 12-month amplitude of precipitation in SEPAR stations grows as precipitation in winter increases. This rise of winter precipitation might well be in part related to the circumpolar vortex expansion by this time which tends to shift strongest westerly flow southwards (Winstanley, 1973a). In contrast, the precipitation summer minimum would deepen. This would seem to offer a somewhat convincing explanation for the divergence in trends between annual DAPA and SEPAR annual amplitudes. On the other hand, concerning the semiannual component, SEPAR station variabilities present some spatial structure on a broader or more regional scale than SEPMER and hybrid stations, which are on a more localized scale. Furthermore, a significant decreasing trend is evident for the SEPAR and hybrid-station amplitudes, whereas no unique trend in sign is detected within the SEPMER region. Broadly speaking, a change in the seasonal distribution of most southwestern Europe (SEPAR) stations emerges as a positive significant trend for the 12-month component, as well as a negative significant trend for the

semiannual component. In contrast, SEPMER stations do not show such uniform behaviour.

The relationship between the annual component of precipitation in most of the southwestern Europe region and sea-level pressure gradient over the northern Atlantic Ocean seems to be relevant. It would be interesting to assess whether the general downward trend in the strength of the seasonal zonal circulation since the late 1920s will continue in the near future. Therefore, much additional work is needed to examine further the relevance of these results on the seasonal distribution of precipitation and to clarify the mechanisms of the Atlantic interannual forcing on seasonal variability.

Acknowledgements. We owe a great deal of thanks to the Instituto Nacional de Meteorología (INM) de España, to CDIAC, to C. Merlier (Météo-France) and to Dr. P. D. Jones for providing the data. We would like to thank Dr. P. Restrepo for encouraging this research and Dr. P. Cuesta for technical support. We also thank the two anonymous referees for their valuable comments on this paper. Some of the figures were drawn by Y. Luna and M. L. Martín. This research was made possible through financial support from the Comunidad Autónoma de Madrid, Spain under Grants Orden 316/92.

Topical Editor L. Eynard thanks T. Lebet and S. Palmiers for their help in evaluating this paper.

References

Bloomfield, P., *Fourier Analysis of Time Series: An Introduction*, Wiley, New York, 1976.

Bradley, R. S., H. F. Díaz, J. K. Eischeid, P. D. Jones, P. M. Kelly, C. M. Goodess, Precipitation fluctuations over northern hemisphere land areas since the mid-19th century, *Science*, **237,** 171–175, 1987.

Díaz, H. F., R. S. Bradley, and J. K. Eischeid, Precipitation fluctuations over global land areas since the late 1800s, *J. Geophys. Res.*, **94,** 1195–1210, 1989.

Enting, I. G., The interannual variation in the seasonal cycle of carbon dioxide concentration at Mauna Loa, *J. Geophys. Res.*, **92,** D5, 5497–5504, 1987.

Flohn, H., A. Kapala, H. R. Knoche, and H. Machel, Recent change of the tropical water and energy budget and of mid-latitude circulations, *Clim. Dyn.*, **4,** 237–252, 1990.

Hsu, C. F., and J. M. Wallace, The global distribution of the annual and semiannual cycles in precipitation, *Mon. Weather Rev.*, **104,** 1093–1101, 1976.

Humphries, J. W., and P. J. Restrepo, Demodulation-remodulation revisited: theory and application, *Water Resour. Res.*, **28,** 1823–1831, 1992.

Lamb, P. J., and R. Peppler, North Atlantic oscillation: concept and application, *Bull. Am. Meteorol. Soc.*, **68,** 1218–1225, 1987.

Loewe, F., A period of warm winters in western Greenland and the temperature see-saw between western Greenland and central Europe, *Q. J. R. Meteorol. Soc.*, **63,** 365–372, 1937.

Maheras, P., Changes in precipitation conditions in the western Mediterranean over the last century, *J. Climatol.*, **8,** 179–189, 1988.

Makrogiannis, T. J., H. S. Sahsamanoglou, A. A. Flocas, and A. Bloutsos, Analysis of the monthly zonal index values and long-term changes of circulation over the North Atlantic and Europe, *Int. J. Climatol.*, **11,** 493–503, 1991.

Manley, G., Central England temperatures: monthly means 1659 to 1973, *Q. J. R. Meteorol. Soc.*, **100,** 389–405, 1974.

Pfister, C., Monthly temperature and precipitation in central Europe 1525–1979: quantifiying documentary evidence on weather and its effects, in *Climate Since A. D. 1500*, eds. R. S. Bradley and P. D. Jones, Routledge, London, 118–142, 1992.

Rogers, J. C., The association between the North Atlantic oscillation and the southern oscillation in the northern hemisphere, *Mon. Weather Rev.*, **112,** 1999–2015, 1984.

Smith, S. G., Changes in the seasonal variation of temperature over the United Kingdom between 1861 and 1980, *Meteorol. Mag.*, **113,** 16–24, 1984.

Snedecor, G. W., and W. G. Cochran, *Statistical Methods*, Iowa State Univ. Press, Iowa, 6th Ed., 1967.

Tabony, R. C., Non-sinusoidal features of the seasonal variation of temperature in mid-latitudes, *Meteorol. Mag.*, **113,** 64–71, 1984.

Thompson, R., Complex demodulation and the estimation of the changing continentality of Europe's climate, *Int. J. Climatol.*, **15,** 175–185, 1995.

Thomson, D. J., The seasons, global temperature, and precession, *Science*, **268,** 59–68, 1995.

Trenberth, K. E., Some effects of finite sample size and persistence on meteorological statistics. Part I: autocorrelations, *Mon. Weather Rev.*, **112,** 2359–2368, 1984.

Valero, F., J. A. García-Miguel, M. L. Martín, and Y. Luna, Detecting long-term variations in precipitation in the southeastern Iberian Peninsula, *Ann. Geophysicae*, **11,** 837–845, 1993.

Valero, F., J. F. González, F. J. Doblas, and J. A. García-Miguel, A method for the reconstruction and temporal extension of climatological time series, *Int. J. Climatol.*, **16,** 213–227, 1996.

Villa, D., J. Guerra, and R. Corres, *Análisis Estadístico de la Pluviometría en la Península Ibérica*, Publ. A-132 INM, Madrid, 1985.

Winstanley, D., Recent rainfall trends in Africa, the Middle East and India, *Nature*, **243,** 464–465, 1973a.

Winstanley, D., Rainfall patterns and general atmospheric circulation, *Nature*, **245,** 190–194, 1973b.